Kinetics and adsorption behaviour of benzoate and phthalate at the α-alumina–water interface: Influence of functionality

Manash R. Das, Sekh Mahiuddin *

Material Science Division, Regional Research Laboratory, Jorhat 785006, Assam, India

Abstract

A systematic study on the influence of functionality on adsorption of benzoate and phthalate at α-alumina–water interface was investigated. Kinetics of adsorption of benzoate and phthalate on α-alumina surfaces were performed at constant ionic strength, $I = 5 \times 10^{-4}$ mol dm^{-3} and pH 5 at 25, 30 and 40 °C. Kinetics results show that the rate of adsorption of phthalate is ≈2 times more than that of benzoate on α-alumina surfaces at 25 °C. The adsorption of benzoate and phthalate on α-alumina surfaces were carried out over a wide range of concentration of adsorbate at fixed ionic strength, $I = 5 \times 10^{-4}$ mol dm^{-3} and pH 5–10. The adsorption isotherms for both the systems were found to be Langmuir in nature. The maximum adsorption density of phthalate is 1.1–5.1 times more than that of benzoate on the same adsorbent under similar condition. This difference is attributed to the presence of adjacent −COOH group in phthalate. The activation energy for both the systems was calculated using Arrhenius equation. The other thermodynamics parameters like Gibbs free energy, enthalpy and entropy were also calculated. The solubility of α-alumina in presence of benzoate and phthalate was found to be depended on the pH of the medium and the concentration of sodium chloride. The surface complexation of benzoate and phthalate on α-alumina surfaces were investigated using the Fourier transform infrared (FTIR) spectroscopy. Benzoate forms outer-sphere complexes with α-alumina surfaces at pH 5 and 6 depending on the shifting of the asymmetric and symmetric bands. Whereas phthalate forms both outer- and inner-sphere surface complexes with α-alumina surfaces.

© 2005 Elsevier B.V. All rights reserved.

*Keywords:* Adsorption isotherm; α-Alumina; Benzoate; FTIR; Kinetics; Phthalate; Zeta potential

1. Introduction

The chemical reaction occurring at the metal oxide–water interface is of great importance in geochemistry and mineral processing industries. The surface hydroxyl groups of metal oxide surfaces are amphoteric in nature, where surface ionization reaction takes place depending on the pH of the aqueous medium.

Protonation:

$$S–OH + H^+ \rightarrow S–OH_2^+$$

Deprotonation:

$$S–OH \rightarrow S–O^- + H^+$$

$$\text{or } S–OH + OH^- \rightarrow S–O^- + H_2O$$
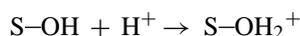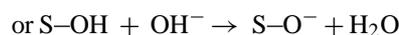
Due to surface ionization, metal oxide exhibits Lewis acid base character [1] and behaves as an adsorbent because of its strong interaction with an adsorbate through surface hydroxyl group. Aluminium oxide and aluminium (oxy)hydroxide also show both Brönsted and Lewis acid base character [2,3]. α-Alumina surfaces interact with water creating a numbers of hydroxyl surface sites with different binding energy [4,5]. It was also reported that α-alumina surfaces converted into a mixture of bayerite and gibbsite when it contact with water at least for 1 h [5,6].

* Corresponding author. Tel.: +91 376 2370081; fax: +91 376 2370011.
E-mail address: mahirrljt@yahoo.com (S. Mahiuddin).

The organic compounds with carboxyl (−COOH) group are commonly found in nature and are important for industrial and geochemical processes. Humic acid is one of the examples found in soil and surface and ground water [7,8], which contains condensed aromatic rings with predominantly −COOH and −OH groups and is effective surface-active agent [9] for beneficiation of hematite from their mineral mixture. Sodium humate is selectively adsorbed on the hematite surfaces and flocculated from their mineral mixture [10,11]. Humic substances (both humic and fulvic acid) are supra molecular in nature and contain condensed aromatic rings with −COOH and −OH groups. Pyrolysis gas-chromatography/mass spectroscopy studies showed that fulvic acid contains more −COOH groups compared to humic acid [12]. Recently, Plancque et al. [13] reported the molecular structure of fulvic acid using electrospray ionization mass spectrometry and suggested that aromatic rings with −COOH and −OH groups are the building blocks of fulvic acid. The low molecular weight aromatic anions like benzoate, phthalate and salicylate are considered to be the model molecules for humic substances. Therefore, depending on the structure, functionality and the conformational factors, the adsorption profile and the surface complexation are different [14,15]. Due to the complex nature of the humic acid or its salt, model molecules with well defined structure like benzoic, salicylic and phthalic acids and the like one with different polydispersibility and polyfunctionality are being chosen for studying adsorption and complexation behaviour on different metal oxides surfaces. A good amount of work has appeared in the literature for adsorption of small organic anions [16–27] and humate [28,29] on the aluminium oxide and aluminium (oxy)hydroxide surfaces.

Gu et al. [30] and Evanko and Dzombak [14,15] studied the adsorption behaviour of small aromatic organic acids on metal oxide surfaces and suggested possible surface complexations through carboxylic and phenolic groups depending on the functionality and polydispersibility of small aromatic acids. The results also showed that the extent of adsorption of simple aromatic acids with different functionality on the goethite in aqueous medium was different. For example, the amount of carboxylic acids adsorbed on the goethite under similar experimental conditions are in the order of mellitic acid (benzene hexacarboxylic acid) > pyromellitic acid (benzene-1,2,4,5-tetracarboxylic acid) > trimellitic acid (benzene-1,2,4-tricarboxylic acid) > phthalic acid (benzene-1,2-dicarboxylic acid) > benzoic acid (benzenecarboxylic acid) [14]. Similarly, adsorption of phthalate, salicylate and p-hydroxybenzoic acids on the iron oxide surfaces showed that an adjacent −COOH group greatly influence the adsorption density than that of −OH group adjacent to −COOH group and at para position [30].

Spectroscopic studies revealed the interaction patterns of simple organic acids with oxide mineral surfaces and the possibility of different surface complexes. Based on the shifting of $\nu_{as}(COO^-)$ and $\nu_s(COO^-)$ bands of benzoate after adsorption on bayerite and comparing the corresponding peak frequency of benzoate–aluminium complex in solution, Phambu [23] concluded that the benzoate forms bidentate bridging complex with the bayerite surfaces. Koutstaal and Ponec [31] also compared the shifting of $\nu_{as}(COO^-)$ and $\nu_s(COO^-)$ bands of benzoate after adsorption on the γ-Al$_2$O$_3$ surfaces with that of corresponding peak frequency of sodium benzoate and suggested that the surface complexation was probably due to the bridging. Phthalate forms different type of surface complexes either outer-sphere [18,22] or both outer- and inner-sphere [25,26] complexes with aluminium oxide, aluminium (oxy)hydroxide and goethite depending on the pH and ionic strength of the medium.

Further, the state of equilibrium of the adsorption of small organic anion on metal oxide surfaces depends on the functionality of the adsorbate molecule. Earlier, it has been reported that the state of equilibrium for natural hematite–benzoate system was obtained after 144 h in comparison to the natural hematite–salicylate system where it was 70 h [32]. Influence of the structural features on the kinetics and adsorption of small aromatic acids on the alumina and aluminium oxy(hydroxide) is not rich in the literature. However, Kummert and Stumm [16] have reported the adsorption of benzoate on γ-alumina as a function time but the kinetics and thermodynamics parameters have not been reported.

In continuation of our studies [27,32], the aim of the present investigation is to compare the adsorption kinetics at a fixed pH, adsorption isotherms at different pH values, effect of ionic strength on the adsorption and the nature of the surface complexation of the benzoate and phthalate at the α-alumina–water interfaces.

2. Experimental

2.1. Material

α-Alumina (>99.7%, Aldrich, Germany) was washed twice with distilled water, dried and finally reactivated at ≈700 °C. Sodium benzoate (>99.5%, E. Merck, India), phthalic acid (>99.5%, E. Merck, India), sodium hydroxide (LR grade, S.D. Fine-Chem, India), sodium chloride (AR grade, E. Merck, India) and hydrochloric acid (AR grade, NICE Chemicals, India) were used without further purification. Disodium phthalate was prepared from the reaction of phthalic acid with sodium hydroxide maintaining pH 7.3.

2.2. Adsorbent

Differential thermal analysis (DTA) and thermogravimetric analysis (TGA) (SDT 2960, TA Corporation, USA) and Fourier transform infrared (FTIR) (model-2000, Perkin-Elmer, USA) spectra of activated α-alumina were recorded and the results shows that the alumina contains predominately α-phase. The zeta potential of the adsorbent at different concentrations of NaCl and pH was measured using Zetasizer-3000HS (Malvern Instruments, UK). The pH of the

suspension of adsorbent at a fixed ionic strength was initially adjusted at ≈ 3.0 and the zeta potential was measured with increase in pH of the suspension by adding dilute sodium hydroxide with a multipurpose titrator (DTS 5900, Malvern, UK). The zeta potential was measured at $25\,^\circ$C and controlled by a PCS software provided by Malvern Instruments, UK. The specific surface area was determined by BET method and was found to be $7.29\,\mathrm{m^2\,g^{-1}}$.

2.3. Adsorption kinetics

The adsorption density of benzoate and phthalate separately on α-alumina (0.5 g) in a 15 mL suspension at pH 5 and ionic strength, $I = 5 \times 10^{-4}\,\mathrm{mol\,dm^{-3}}$ NaCl in a batch process was measured as a function of time at different temperatures. The suspensions at different interval of time were cooled and centrifuged at 12,500 rpm for 15 min (relative centrifugal force $= 28,790 \times g$). The residual concentration of benzoate and phthalate was estimated at $\lambda_{\max} = 224.6$ and 273 nm (absorption maximum), respectively, with a UV–visible spectrophotometer, Specord 200 (Analytik Zena, Germany). The amount of adsorbate adsorbed per unit surface area of the adsorbent (adsorption density) was estimated by mass balance using the following relation:

$$\Gamma = \frac{(C_0 - C_e)V}{ma} \tag{1}$$

where, C_0 and C_e are the initial and residual concentration of the adsorbate in the suspension, V the volume of the suspension and m and a are the mass and surface area of the adsorbent, respectively.

2.4. Adsorption isotherm

Adsorption of benzoate and phthalate on the α-alumina was carried out at 25 and $30\,^\circ$C, respectively, in a screw-capped glass tube. A suspension of 15 mL containing 0.5 g α-alumina and $5 \times 10^{-4}\,\mathrm{mol\,dm^{-3}}$ NaCl solution was mixed thoroughly with the help of a vortex mixer. The pH of the suspension was adjusted to a desired value within ± 0.1 units using either NaOH or HCl solution and then allowed to equilibrate for 1 h. The required amount of sodium benzoate or sodium phthalate was added and the pH of the suspension was readjusted, if necessary. The suspension was then allowed to equilibrate with intermittent mixing for 48 and 20 h (duration of equilibrium adsorption test for benzoate and phthalate, respectively). After the equilibration, the suspension was then centrifuged and the residual concentration of benzoate and phthalate was estimated.

2.5. Dissolution of α-alumina

The influence of background electrolyte, NaCl, on the solubility of α-alumina in the presence of benzoate and phthalate at a fixed concentration of $2.0\,\mathrm{mmol\,dm^{-3}}$, selected pH

and at $25\,^\circ$C was studied. For the purpose, adsorption of benzoate and phthalate at different concentrations of NaCl was carried out upto the respective equilibration time as followed for adsorption isotherms. The concentration of the sodium chloride was varied from 0 to $10\,\mathrm{mmol\,dm^{-3}}$. After the equilibration time, the suspension was centrifuged and the dissolved Al^{3+} in the supernatant liquid was estimated by Atomic Absorption Spectrophotometer, Spectraa 220 (Varian, Australia), using aluminium flame and N_2O/acetylene gases at lamp current 10 mA and wavelength 309.3 nm.

2.6. FTIR spectroscopy

For FTIR studies, 0.5 g of the α-alumina was equilibrated with $0.01\,\mathrm{mol\,dm^{-3}}$ sodium benzoate and $0.001\,\mathrm{mol\,dm^{-3}}$ phthalate at a desired pH maintaining ionic strength, $I = 5 \times 10^{-4}\,\mathrm{mol\,dm^{-3}}$ NaCl following the same procedure adopted for adsorption. The suspension was centrifuged and the residue was washed with distilled water once, centrifuged and dried in a vacuum desiccator over fused calcium chloride. The pellets were prepared using 2 mg of the sample in 200 mg of spectrograde KBr. The FTIR spectra were recorded with a Perkin-Elmer FTIR spectrophotometer, model 2000 using spectrum 3.2 software. The spectral resolution was $4\,\mathrm{cm^{-1}}$. In the mid infrared region, assignment and identification of peaks after adsorption of benzoate or phthalate on α-alumina for symmetric and asymmetric $-COO^-$ and $C-C$ of aromatic ring vibrations are very difficult due to adsorption of water. In the present study, we subtracted the references FTIR spectra (KBr and α-alumina) from the spectra of the adsorbed benzoate or phthalate using spectrum software.

3. Results and discussion

3.1. Zeta potential

The zeta potential of the α-alumina powder at different ionic strengths are depicted in Fig. 1. The isoelectric point (IEP) of α-alumina in the present investigation is found to be 6.7 without NaCl, which was lowered by 0.3 units in presence of sodium chloride up to $0.005\,\mathrm{mol\,dm^{-3}}$. The small shift in IEP is due to the specific adsorption of Cl^- on the α-alumina surfaces [33]. The present IEP of α-alumina is ≈ 2.5 units lower than the reported value [34–36]. The reason for lowering the IEP of α-alumina is that there is less number of surface hydroxyl groups. Moreover, proton of the surface hydroxyl group is not bound strongly to the oxygen due to little unsatisfied electronegativity of the surface hydroxyl group [35]. Therefore, the proton is easily removed in the lower pH range. The IEP of α-alumina also depend on the medium of storage [37]. The adsorption site concentration as determined by following the procedure of Hohl and Stumm [38] is estimated to be TOT ($\equiv$ AlOH) $= 1.815\,\mathrm{mmol\,dm^{-3}}$ based on the site density of $4.54\,\mathrm{site\,nm^{-2}}$, which is less than the reported
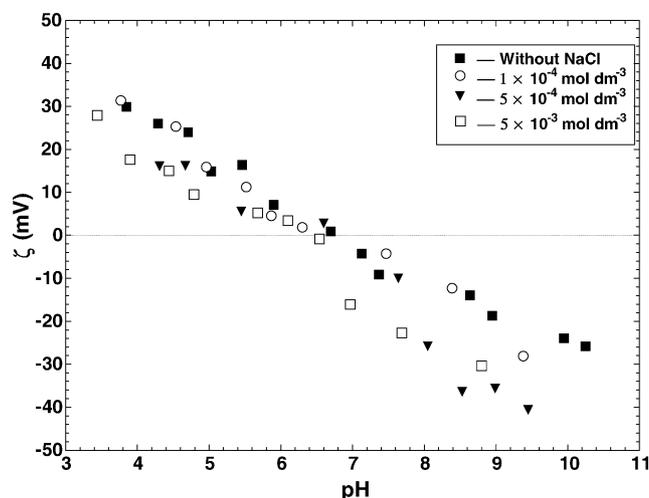
Fig. 1. Variation of zeta potential of α-alumina with pH at different concentrations of NaCl at 25 °C (initial pH of the suspension was adjusted at ≈3.0).

site density of α-alumina [27] and is also responsible for the lower IEP in the present adsorbent.

3.2. Kinetics of adsorption of benzoate and phthalate

The amount of benzoate and phthalate adsorbed per unit surface area of α-alumina at different temperatures is shown in Figs. 2 and 3, respectively. It is apparent from Fig. 2 that the state of equilibrium for adsorption of benzoate at the α-alumina–water interface is attained at 30 h within the temperature range of study. Kummert and Stumm [16] reported 6 h to attain the equilibrium for adsorption of benzoate on γ-alumina surfaces. This difference may be due to surface loading and the nature of adsorbent. An equilibration time of 48 h was chosen for adsorption study. In the case of phthalate–α-alumina system (Fig. 3), adsorption density of phthalate on α-alumina surfaces increases up to 20–25 h at 30 and 40 °C,
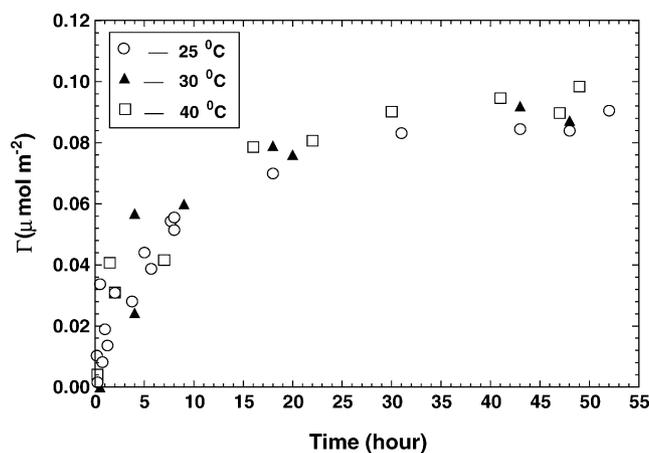

Fig. 2. Effect of temperature on the adsorption of benzoate on α-alumina surfaces at fixed initial concentration of sodium benzoate: $C_0 = 2 \times 10^{-4}$ mol dm^{-3}, α-alumina = 0.5 g, $I = 5 \times 10^{-4}$ mol dm^{-3} NaCl, $V = 15$ mL and pH = 5.0.
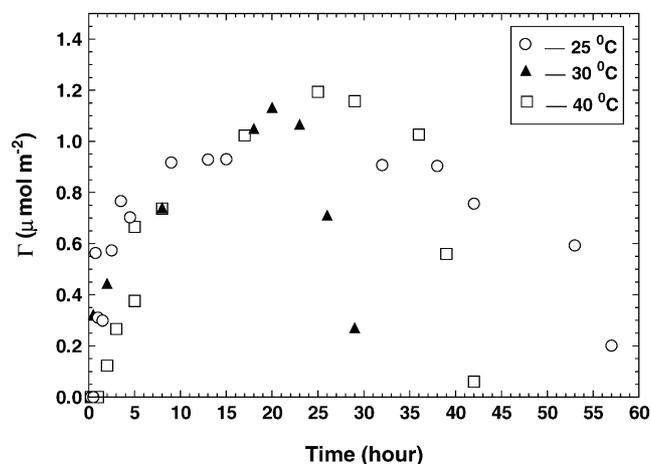

Fig. 3. Effect of temperature on the adsorption of phthalate on α-alumina surfaces at fixed initial concentration of phthalate: $C_0 = 2 \times 10^{-4}$ mol dm^{-3}, α-alumina = 0.5 g, $I = 5 \times 10^{-4}$ mol dm^{-3} NaCl, $V = 15$ mL and pH = 5.0.

after that it decreases as reaction time increases. But at 25 °C, state of equilibrium is attained at 10 h and beyond 37 h, adsorption density decreases. Unlike benzoate–α-alumina system, the decrease in Γ after attaining the plateau for phthalate–α-alumina system is linked with the dissolution of α-alumina at pH 5. A similar dissolution of corundum outside the $5 < \text{pH} < 9$ has been reported [39]. Preliminary study shows that the dissolution of α-alumina critically depends on the pH, temperature and concentration of phthalate. The concentration limit of phthalate at different pH beyond which α-alumina starts to dissolve is ≈1.0 mmol dm^{-3}.

The kinetics parameter, k is the rate constant for adsorption, was estimated using the following equation [40]:

$$\frac{1}{C(t)} = \frac{kt}{C_0} + \frac{1}{C_0} \qquad (2)$$

where, C_0 and $C(t)$ are the initial concentration and the concentration at time t of the adsorbate. The estimated values of the k parameter for benzoate–α-alumina system and phthalate–α-alumina system are given in Table 1 along with the values of the adsorption coefficient (K_s) at different temperatures, as obtained by using Langmuir equation, which is outlined in Section 3.3. The rate of adsorption of benzoate and phthalate on α-alumina increases with the increase in temperature. The calculated value of k parameter from the

Table 1
Values of the adsorption coefficient (K_s) and the rate constant (k) for benzoate and phthalate adsorption on α-alumina

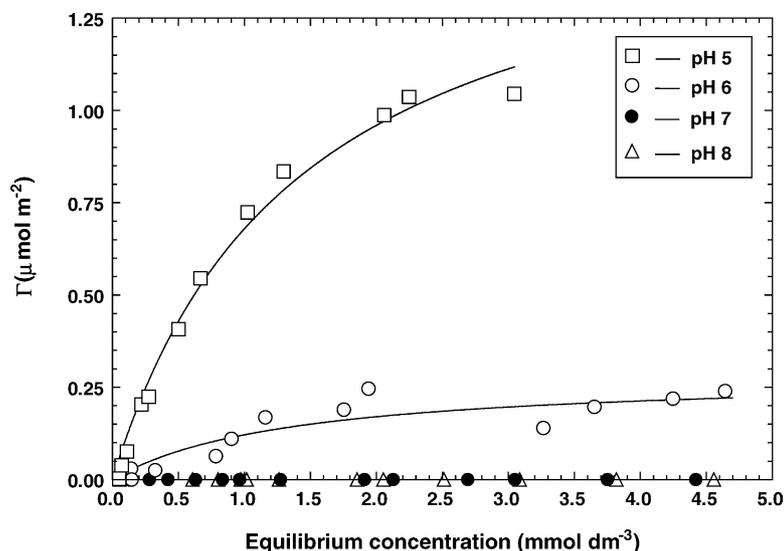| Temperature (°C)	K_s	k (h^{-1})
Benzoate		
25	0.71	1.91×10^{-3}
30	0.83	2.17×10^{-3}
40	0.94	4.05×10^{-3}
Phthalate		
25	80.8	4.14×10^{-3}
30	89.9	6.95×10^{-3}
40	215.9	8.31×10^{-3}

Fig. 4. Adsorption isotherms of benzoate onto α-alumina at different pH, fixed $I = 5 \times 10^{-4}$ mol dm^{-3} NaCl, α-alumina = 0.5 g, V = 15 mL and at 25 °C. Symbols are experimental and the solid lines are the theoretical value (Eq. (3)), respectively. The data points represent triplicate adsorption experiments.

reported data of adsorption of benzoate on γ-alumina [16] at 22 °C was 2.97×10^{-3} h^{-1}, which is ≈1.5 times more than the present benzoate–α-alumina system at 25 °C. This difference is due to nature of the adsorbent, particularly the less number of surface hydroxyl group in α-alumina. The rate constant for adsorption of phthalate on α-alumina surfaces, k is ≈2 times more than that of benzoate on the same adsorbent. The higher value of the K_s parameter (Table 1) suggest that the adsorption of phthalate on α-alumina, in comparison to benzoate, is more favourable, which is due to the presence of one adjacent carboxylic group in phthalate.

3.3. Adsorption isotherm

The adsorption isotherms for benzoate–α-alumina system and phthalate–α-alumina system at a fixed ionic strength, $I = 5 \times 10^{-4}$ mol dm^{-3} NaCl, different pH and 25 and 30 °C are shown in Figs. 4 and 5, respectively. Adsorption isotherms of benzoate–α-alumina systems show that adsorption increases with increase in the concentration of benzoate and ultimately a plateau is reached. The adsorption density of benzoate decreases sharply as the pH of the suspension increases. It is reflected in the pH range 5 and 6, which is accounted for the decrease in the surface positive charge of α-alumina. At pH 7 and onwards (above IEP = 6.7), there is no detectable benzoate adsorption on the α-alumina surfaces, which is due to the surface charge reversibility.

In the case of phthalate–α-alumina systems, we restricted the initial phthalate concentration up to 1.0 mmol dm^{-3}, since dissolution from α-alumina surface occurs beyond this concentration. The adsorption density plots (Fig. 5) show that the adsorption increases with the increase in phthalate concentration within the pH range of the study and finally a plateau is reached. To ascertain the dissolution of α-alumina, we conducted similar adsorption experiments at different pH

values, as outlined in Section 2, using higher concentration of benzoate and phthalate (>1.0 mmol dm^{-3}). The supernatant liquids for phthalate–α-alumina system exhibit positive test with dilute ammonium hydroxide. Such dissolution is due to the fact that one of the functional carboxylic groups of phthalate is not ionized below pH 7.3 and the bonding patterns between phthalate and α-alumina surfaces is different, which is responsible for dissolution.

The adsorption isotherms (Figs. 4 and 5) for both the systems are Langmuirian in nature. Therefore, the Langmuir adsorption isotherm equation of the following form was used to fit the experimental adsorption data:
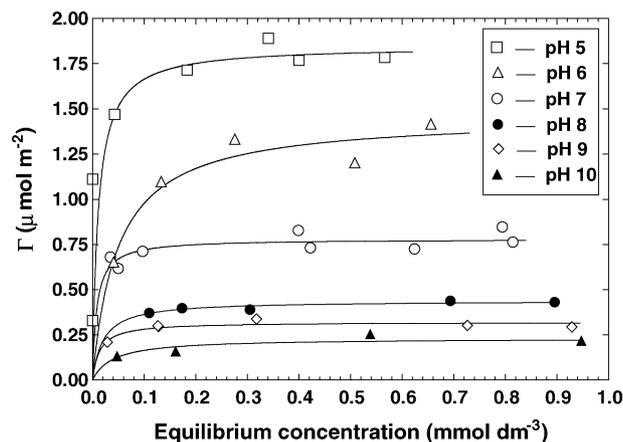
$$\Gamma = \Gamma_{max} \frac{C_e}{(K + C_e)} \tag{3}$$

Fig. 5. Adsorption isotherms of phthalate onto α-alumina at different pH, fixed $I = 5 \times 10^{-4}$ mol dm^{-3} NaCl, α-alumina = 0.5 g, V = 15 mL and at 30 °C. Symbols are experimental and the solid lines are the theoretical value (Eq. (3)), respectively. The data points represent triplicate adsorption experiments.

Table 2
Values of the parameters of Eq. (3) as function of pH for benzoate and phthalate adsorption on α-alumina surfaces

Langmuir parameters	pH					
	5	6	7	8	9	10
Benzoate						
Γ_{max} (μmol m^{-2})	1.634	0.285				
K_s	0.71	0.74				
Standard deviation	0.044	0.034				
Phthalate						
Γ_{max} (μmol m^{-2})	1.849	1.458	0.780	0.438	0.320	0.229
K_s	89.93	20.32	121.5	48.40	70.87	24.97
Standard deviation	0.475	0.166	0.126	0.148	0.019	0.028

where, C_e is the equilibrium concentration of adsorbate in mmol dm^{-3}, $K = 1/K_s$, K_s the adsorption coefficient and Γ and Γ_{max} are the concentrations of the adsorbate in μmol m^{-2} at equilibrium and after saturation of the α-alumina surface, respectively. The values of Γ_{max} and K_s are presented in Table 2 along with the standard deviations. For benzoate–α-alumina system, the Γ_{max} value at pH 6 is ≈5 times lower than at pH 5 (Table 2) and no adsorption of benzoate on α-alumina at pH 7 and onwards was observed. Such a change in Γ_{max} is expected as the positive surface site decreases as the pH increases. Moreover, the IEP of α-alumina is 6.7. Therefore, benzoate has a less tendency to form surface complexes on the neutral surface of α-alumina (≡AlOH surf). In the case of phthalate–α-alumina system, Γ_{max} decreases sharply with the increase in pH up to 8, thereafter Γ_{max} decreases gradually.

Unlike benzoate–α-alumina system, the higher value of Γ_{max} and the variation of Γ_{max} with pH for phthalate–α-alumina system is due to: (a) the adjacent carboxylic group enhances the adsorption density [15] and (b) higher adsorption density beyond IEP = 6.7 in comparison to benzoate is due to the ionization of second carboxylic group and bonding patterns with the available ≡AlOH surface.

The adsorption density of salicylate [27] and benzoate and phthalate (this study) on α-alumina at pH 5 and 6 shows contradictory trend of functionality. So, to investigate the influence of the functionality, an alternative approach is to consider the value of K_s, which is also a key parameter for measuring the magnitude of adsorption. So, we consider the value of the K_s parameter of salicylate [27] and benzoate and phthalate (Table 2). The K_s value follows the sequence: benzoate < salicylate < phthalate, which clearly shows that an additional −COOH group in ortho position in phthalate enhances the adsorption density than the −OH in ortho position in salicylate.

3.4. Variation of ionic strength

The adsorption density of benzoate and phthalate on α-alumina surface at 25 and 30 °C with the increase in concentration of background electrolyte, sodium chloride, at different pH and constant initial concentration of adsorbate ($C_0 = 2 \times 10^{-3}$ mol dm^{-3}) is depicted in Figs. 6 and 7,

respectively. It is apparent from Fig. 6 that the adsorption density of benzoate decreases by ≈0.25 μmol m^{-2} as the ionic strength increases from 0.05 to 10 mmol dm^{-3}. But the effect of ionic strength is not observed at pH 6. At around
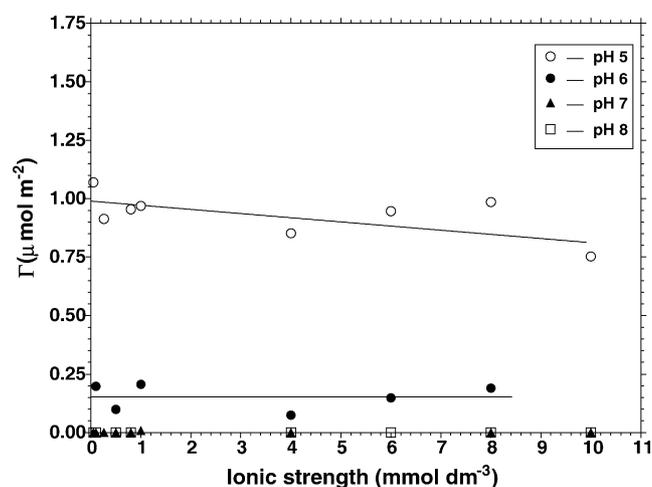

Fig. 6. Variation of adsorption density of benzoate on α-alumina with ionic strength at different pH values and 25 °C, $C_0 = 2 \times 10^{-3}$ mol dm^{-3}, α-alumina = 0.5 g and V = 15 mL.

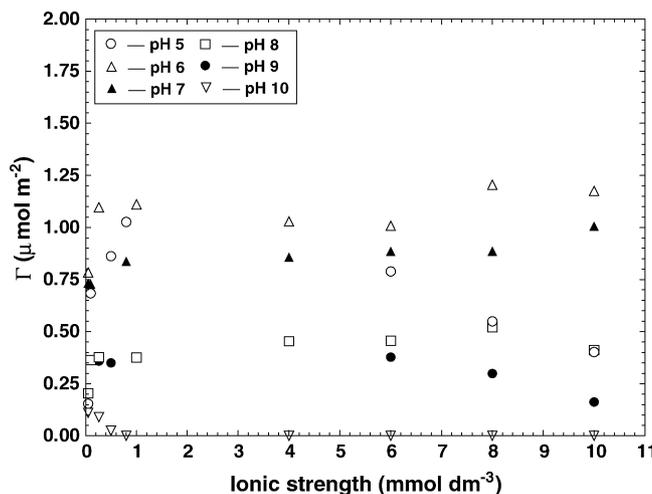Fig. 7. Variation of adsorption density of phthalate on α-alumina with ionic strength at different pH values and 30 °C, $C_0 = 2 \times 10^{-3}$ mol dm^{-3}, α-alumina = 0.5 g and V = 15 mL.
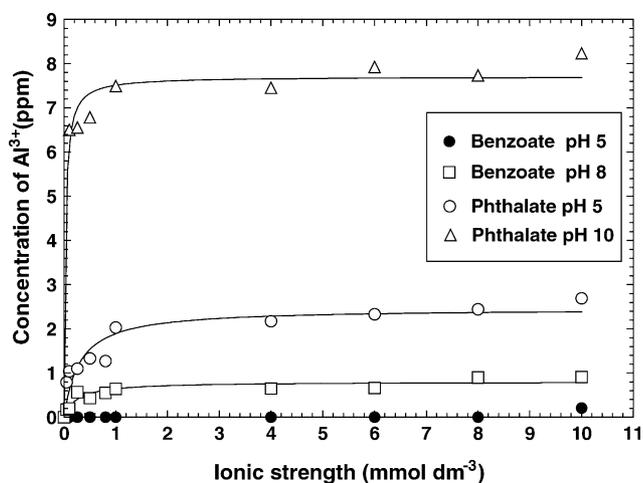
Fig. 8. Dissolution of α-alumina in presence of benzoate and phthalate with ionic strength at different pH values and 25 °C, $C_0 = 2 \times 10^{-3}$ mol dm^{-3}, α-alumina = 0.5 g and $V = 15$ mL.

IEP = 6.7 and above, sodium chloride has no influence on the adsorption of benzoate on the α-alumina surfaces. Fig. 7 shows that the adsorption density of phthalate attains maximum at 0.8 mmol dm^{-3} NaCl from pH 5 to 8 and it is decreased by 0.6 μmol m^{-2} as the ionic strength increase up to 10 mmol dm^{-3}. But beyond 0.8 mmol dm^{-3}, there is no influence of NaCl on the adsorption density from pH 6 to 8. At pH 9, adsorption density is decreased by ≈0.2 μmol m^{-2} whereas at pH 10, adsorption density decreases with the increase in ionic strength up to 0.8 mmol dm^{-3} and no adsorption is observed at higher ionic strength. It implies that the adsorption of phthalate on α-alumina surface is influenced by ionic strength depending on the pH of the medium. Such a variation in adsorption density is due to the decrease in positive surface potential [41] and the distribution of chloride ions near the surface of α-alumina increases resulting in decrease in thickness of the double layer.

3.5. Dissolution of α-alumina surfaces

The concentration of Al^{3+} in the supernatant liquid after treating with benzoate and phthalate at a concentration of 2×10^{-3} mol dm^{-3} as a function of ionic strength at two pH values is shown in Fig. 8. For benzoate at pH 5, there is no detectable Al^{3+} in the solution except at 10 mmol dm^{-3} NaCl

and the concentration was found to be 0.21 ppm (0.0063 mg/g of α-Al$_2$O$_3$). The concentration of Al^{3+} in the supernatant liquid at all other pH values increases with the increase in NaCl concentration and finally a plateau was obtained exhibiting Langmuir pattern. A similar variation of NaCl induced dissolution of silica has also been reported [42]. Maximum dissolved Al^{3+} in the solution was found to be 0.8 ppm (0.024 mg/g of α-Al$_2$O$_3^-$) for benzoate at pH 8 and 2.5 ppm (0.075 mg/g of α-Al$_2$O$_3$) and 7.6 ppm (0.228 mg/g of α-Al$_2$O$_3$) for phthalate at pH 5 and 10, respectively. The dissolution of α-alumina is greatly influenced by pH of the medium and the concentration of sodium chloride. Reported studies showed that the dissolution of the minerals (aluminium and iron oxides and oxy(hydroxides)) was due to the formation of inner-sphere, bidentate, mononuclear complexes by low molecular weight organic acids/anions [39,43]. In the present study, the dissolution behaviour of α-alumina in the presence of benzoate only at pH 8 and phthalate at pH 5–10 and NaCl envisages the formation of inner-sphere complexes and will be discussed in the subsequent section.

3.6. Thermodynamic parameters

The activation energy for adsorption, E, for both the systems was estimated using Arrhenius equation, $k = Ae^{-E/RT}$, where k is the rate constant for adsorption, A the frequency factor, R the gas constant and T is temperature in Kelvin and the values of other thermodynamic parameters are presented in Table 3. The results imply that the adsorption of benzoate and phthalate on the α-alumina surfaces is endothermic in nature. The activation energy for adsorption of benzoate on α-alumina is ≈1.2 times more than phthalate adsorbed on the same adsorbent. The value of the Gibbs free energy for phthalate–α-alumina system is more negative than that of benzoate on the same adsorbent under similar condition. The thermodynamic results imply that the adsorption of phthalate on the α-alumina is more favourable and easy over benzoate under similar condition due to the presence of one adjacent carboxylic group in phthalate.

3.7. FTIR spectra

The FTIR spectra of benzoate, phthalate and the difference spectra after their adsorption on α-alumina

Table 3
Values of the thermodynamic parameters for adsorption of benzoate and phthalate on α-alumina surfaces at pH 5

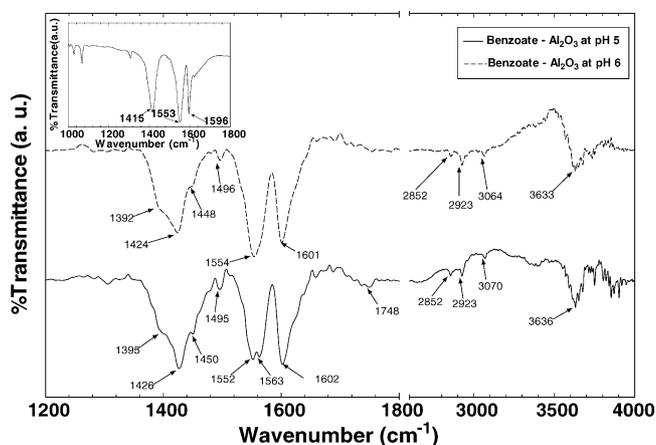| Temperature (K)	E (kJ mol^{-1})	ΔH (kJ mol^{-1})	ΔG (kJ mol^{-1})	ΔS (J mol^{-1} K^{-1})
Benzoate				
298.15			0.843	42.5
303.15	40.3	13.5	0.463	43.1
313.15			0.171	42.7
Phthalate				
298.15			−10.89	215.3
303.15	33.1	53.3	−11.34	213.2
313.15			−13.99	214.8

Fig. 9. FTIR difference spectra of benzoate after adsorption on the α-alumina surfaces at two different pH values (*inset*: FTIR spectra of benzoate).

surfaces at pH 5, 6 and 8 are discussed in the subsequent sections.

3.7.1. Sodium benzoate

The peaks at 1415 and 1553 cm^{-1} (Fig. 9, inset) are assigned to $\nu_s(-COO^-)$ and $\nu_{as}(-COO^-)$ vibrations. The peak at 1596 cm^{-1} is assigned for ν_{c-c} (aromatic) ring. All the characteristics bands of benzoate are given in Table 4 and are in good agreement with the reported band assignment [23,31,44].

3.7.2. Benzoate on α-Al$_2$O$_3$

The peaks for $\nu_{as}(-COO^-)$, $\nu_s(-COO^-)$, ν_{C-O} (phenolic), ν_{C-C} (between aromatic ring and $-COO^-$) and ν_{C-C} (ring) (Table 4 and Fig. 9) are the most important bands for detection and interpretation of surface complexation, on adsorption, of benzoate on the α-alumina surfaces. The characteristic bands for $\nu_s(-COO^-)$ and $\nu_{as}(-COO^-)$ for benzoate after adsorption on α-alumina surfaces are found at 1426 and 1552 cm^{-1} at pH 5 and 1424 and 1554 cm^{-1} at pH 6. The symmetric $(-COO^-)$ and asymmetric $(-COO^-)$ bands resemble with the reported band assignments [23,31,44]. The peak at 1596 cm^{-1} of the ligand spectra (Fig. 9, inset) is found at ≈1601 cm^{-1} (Fig. 9) for both pH is assigned to ν_{c-c} (aromatic) ring. The band at ≈1495 and ≈1450 cm^{-1} are assigned for ν_{c-c} (ring and $-COO^-$). For benzoate–α-alumina system, $\Delta\nu$ ($\Delta\nu = \nu_{as} - \nu_s$ of $-COO^-$) is found to be 126 cm^{-1}

Table 4
Characteristic peak frequencies of benzoate and after adsorption on α-alumina surfaces

Mode	ν (cm^{-1})		
	Benzoate	pH 5	pH 6
ν_s ($-COO^-$)	1415	1426	1424
ν_{as} ($-COO^-$)	1553	1552	1554
ν_{C-C} (ring and $-COO^-$)	1491	1495	1496
		1450	1448
ν_{C-C} (ring)	1596	1602	1601
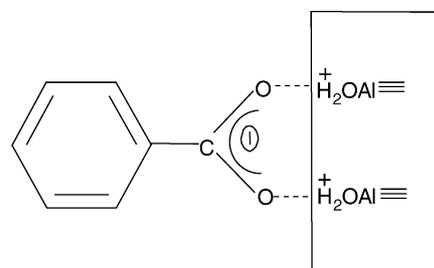
at pH 5 and 130 cm^{-1} at pH 6 (Fig. 9), which are smaller ($\Delta\nu = 138$ cm^{-1}) than that of noncomplexed form (ionic, Fig. 9, inset). The reported $\Delta\nu$ for benzoic acid–aluminium hydroxide (bayerite) [23] and benzoic acid–γ-alumina [31] systems is ≈158 and 116 cm^{-1}, respectively. The magnitude $\Delta\nu$ has been considered for identification for complexes in the case of a simple ligand such as acetate [45]. But this relationship of $\Delta\nu$ with types of complexes has been questioned for carboxylate as a ligand other than acetate [46].

The relative shift of $\nu_s(-COO^-)$ and $\nu_{as}(-COO^-)$ band and the full width at half maximum (fwhm) of the respective stretching frequency are considered for the identification of the surface complexes. The shifting of the $\nu_s(-COO^-)$ to the higher frequency region demonstrates that the benzoate is chemisorbed on the α-alumina surfaces. Nordin et al. [25] proposed outer- and inner-sphere surface complexes considering the shifting of $\nu_s(-COO^-)$ band by ≈20 and ≈46 cm^{-1} to the high frequency region, respectively. On the other hand, the broadening of the $\nu_s(-COO^-)$ and $\nu_{as}(-COO^-)$ bands of the organic carboxylate also favours the formation of outer-sphere surface complexes [24,39]. In the present system, $\nu_s(-COO^-)$ band of benzoate after adsorption shifted by only ≈10 cm^{-1} to higher frequency region from 1415 to 1424–1426 cm^{-1}. A band at 3633 cm^{-1} represents the surface hydroxyl group. Nevertheless, we could not detect dissolved Al^{3+} in the supernatant liquid at pH 5 and 6 and 0.5 mmol dm^{-3} NaCl concentration, which favours the outer-sphere complexes [47–49]. Therefore, with the above results, benzoate forms outer-sphere complexes with the α-alumina surfaces as shown in Fig. 10.

3.7.3. Phthalate

The FTIR spectra of phthalate (disodium salt) exhibit the peaks at 1609, 1486 and 1441 cm^{-1} that are due to ν_{c-c} (aromatic) ring vibrations. Two equivalent carboxylate groups are identified by two symmetric (ν_s) bands at 1388 and 1418 cm^{-1} and two asymmetric bands at 1552 and 1576 cm^{-1} [25]. The bands at 1085 and 1147 cm^{-1} are assigned for $\delta(C-H)$. The band at ≈1704 cm^{-1} due to $\nu(C=O)$ is absent for phthalate. But a weak peak is observed at 1290 cm^{-1} for ν_{C-O}. All characteristic peaks for phthalate are given in Table 5 and resemble with previously reported band assignment [21,26,50].

Fig. 10. Schematic representation of surface complexation of benzoate with α-alumina at pH 5 and 6.

Table 5
Characteristic peak frequencies of phthalate and after adsorption on α-alumina surfaces

Mode	ν (cm^{-1})				
	Phthalic acid	Phthalate	pH 5	pH 6	pH 8
ν_s (−COO$^-$)		1388	1395	1388	1400
		1418	1420	1415	1418
				1422	
ν_{as} (−COO$^-$)		1552	1584	1581	1562
		1576	1563	1565	1574
			1553	1552	
ν_{C-C} (ring)	1584	1609	1611	1619	1616
	1495	1486	1508	1508	1502
	1404	1441	1488	1491	1488
			1447	1449	1447
$\nu_{C=O}$	1688		1687	1688	1693
ν_{C-OH}	1281		1290	1290	1282

3.7.4. Phthalate on α-Al$_2$O$_3$

The characteristics bands for ν_{as}(−COO$^-$), ν_s(−COO$^-$), ν_{C-C} (between aromatic ring and −COO$^-$) and ν_{C-C} (ring) vibrations of phthalate after adsorption at pH 5, 6 and 8 (Figs. 11 and 12) are presented in Table 5. The bands at ≈1611, ≈1508, ≈1488 and ≈1447 cm^{-1} at three pH are assigned for ring (C−C) vibration.

For assigning the structure of adsorbed phthalate on the α-alumina surfaces, first we consider the spectra of phthalic acid and phthalate (disodium salt prepared at pH 7.3). Phthalic acid exhibits bands due to $\nu_{C=O}$ at 1688 and ν_{C-OH} at 1281 cm^{-1}, respectively, without intramolecular hydrogen bonding [46]. In contrast to phthalic acid, phthalate exhibits bands due to ν_{as} and ν_s at around 1552–1576 and 1388–1418 cm^{-1}, respectively, and no significant peaks for $\nu_{C=O}$ and ν_{C-OH} are observed.
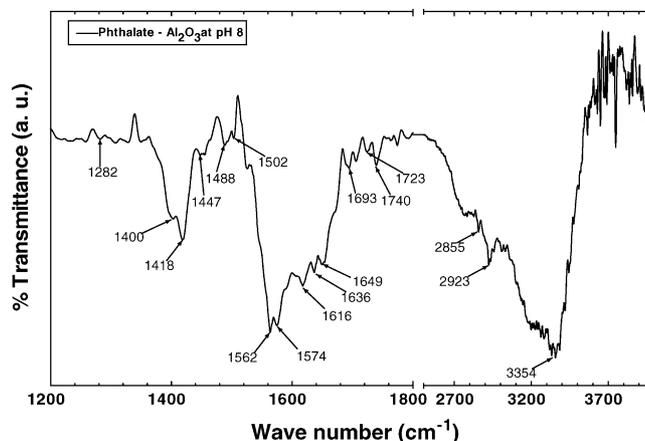

Fig. 12. FTIR difference spectra of phthalate after adsorption on the α-alumina surfaces at pH 8.

The band patterns due to ν_{as}(−COO$^-$) and ν_s(−COO$^-$) after adsorption of phthalate on α-alumina are in accordance with the phthalate–γ-alumina systems [26] and are at higher frequency region with respect to phthalate (ionic form). The difference between ν_{as}(−COO$^-$) and ν_s(−COO$^-$) and the relative shifting and broadening of the asymmetric carboxylic vibrations have been considered for the plausible surface complexation structure of phthalate with alumina or aluminium oxy(hydroxide) surfaces. Nordin et al. [25] suggested both outer- and inner-sphere surface complexes based on the relative intensity of the doublets of ν_s(−COO$^-$).

In comparison to spectra of benzoate and phthalate at pH 5 and 6, weak peak at 1740 cm^{-1} (Fig. 12) for phthalate at pH 8 has appeared and is assigned to $\nu_{C=O}$. The band for ν_{as}(−COO$^-$) and ν_s(−COO$^-$) after adsorption of phthalate on α-alumina appeared at 1563 and 1420 cm^{-1} at pH 5, 1565 and 1415 cm^{-1} at pH 6 and 1562 and 1418 cm^{-1} at pH 8. Significant changes for ν_{as}(−COO$^-$) and ν_s(−COO$^-$)
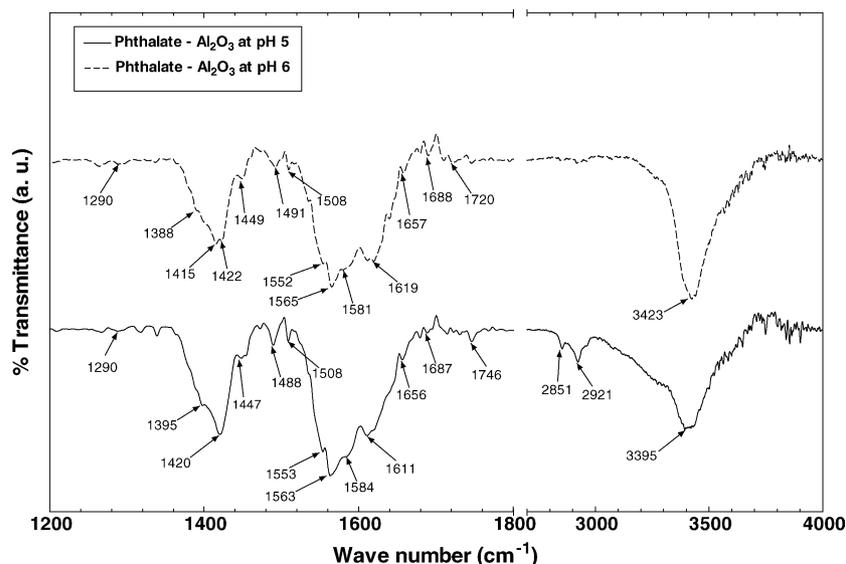

Fig. 11. FTIR difference spectra of phthalate after adsorption on the α-alumina surfaces at two different pH 5 and 6.

band position for phthalate on adsorption has been observed. The relative intensity of two asymmetric and two symmetric bands are changed in comparison to ionic phthalate. Nordin et al. [25] noted such a relative intensity change in $1405\,\mathrm{cm^{-1}}$ over $1422\,\mathrm{cm^{-1}}$ by increasing ionic strength. Gradual increase in intensity in $1405\,\mathrm{cm^{-1}}$ over $1422\,\mathrm{cm^{-1}}$ was due to dominance of inner-sphere complexes over the outer-sphere complexes. As in the case of benzoate–α-alumina systems, the shifting of ν_s band in phthalate–α-alumina system to higher frequency region was also found by same magnitude ($\approx 10\,\mathrm{cm^{-1}}$). In addition to that the ν_{as} is also quite broaden.

Up to pH 7, only one carboxylic group is fully deprotonated. In that case, a strong stretching band at $\approx 1700 \pm 50\,\mathrm{cm^{-1}}$ due to $>\!C\!=\!O$ should appear. Nevertheless, a very weak band at higher frequency region (≈ 1720 and ≈ 1740 at pH 5 and 6) has been observed. We are not sure whether this band is due to $>\!C\!=\!O$ stretching or noise and we are not considering for surface complexation. On the other hand, the absence of a strong band for $>\!C\!=\!O$ in the present system at pH 5 and 6 indicates the presence of intramolecular hydrogen bond [46]. Further, the presence of a broad band at around $3400\,\mathrm{cm^{-1}}$ supports the existence of the intramolecular hydrogen bonding. At pH 5 and 6, the symmetric band at $\approx 1420\,\mathrm{cm^{-1}}$ is relatively stronger than $\approx 1390\,\mathrm{cm^{-1}}$ suggests the presence of inner-sphere complexes [25]. The intramolecular hydrogen bonding, the presence of a broad band at $3400\,\mathrm{cm^{-1}}$ and broading of ν_{as} and ν_s suggest the presence of outer-sphere complexes. Again the dissolution of α-Al$_2$O$_3$ at pH 5 and 6 is caused by the formation of inner-sphere complexes. With the results, it is difficult to assign a surface complexation structure. It seems that both outer- and inner-sphere complexes are co-exit [26]. The presence of inner-sphere complexes polarise and weaken the surface metal–oxygen bonds causing dissolution.

In the pH range 3.7–7.3, phthalate exists as a singly charged anion and beyond pH 7.3 behaves as a doubly charged anion. Therefore, surface complexation of phthalate with α-alumina below and above pH 7.3 will certainly be different.

At pH 8, both the carboxylic groups are ionized and are available for surface complexation. In addition to $\nu_{as}(-COO^-)$ and $\nu_s(-COO^-)$, a weak peak at $1740\,\mathrm{cm^{-1}}$ due to $\nu_{C=O}$ is observed. The relatively intense symmetric band at $1418\,\mathrm{cm^{-1}}$ over $1400\,\mathrm{cm^{-1}}$ suggests the presence of inner-sphere complexes. In this situation, one of the oxygen atoms from both the carboxylate groups are participating in the complex formation [26]. On the other hand, broadening of the asymmetric stretching frequency also suggest the presence of outer-sphere complexes. The dissolution of α-alumina at pH 8 (Fig. 8) is more than that of at pH 5. It seems, the concentration of inner-sphere complexes dominates over the outer-sphere complexes. With the results in hand, it is suggested that the adsorption and mode of surface complexation of benzoate and phthalate on

α-alumina depends on the position of the $-COOH$ groups, pH of the medium and the concentration of the background electrolyte.

4. Conclusions

With the above results, following conclusions can be drawn:

(1) The state of equilibrium in the case of benzoate adsorbed on the α-alumina surfaces at pH 5 in presence of $5 \times 10^{-4}\,\mathrm{mol\,dm^{-3}}$ NaCl is attained at 30 h and almost independent of temperature. Whereas, time required for the state of equilibrium for phthalate–α-alumina system under similar condition is 10 h at 25 °C and temperature dependent.

(2) Adsorption density of phthalate on the α-alumina surfaces is 1.1–5.1 times more than that of benzoate on the same adsorbent under similar experimental condition.

(3) The maximum adsorption density, Γ_{max}, for benzoate–α-alumina system decreases with the increase in pH and becomes zero at pH 6.7, which corresponds to IEP of α-alumina. In the case of phthalate–α-alumina system, Γ_{max} decreases sharply up to the IEP and thereafter it decreases slowly. The results are linked with ionization of second and adjacent $-COOH$ group, which participates in the adsorption by forming surface complexes with the α-alumina surfaces.

(4) Sodium chloride and pH induce the solubility of α-alumina in the presence of phthalate whereas sodium chloride in presence of benzoate has no effect on the solubility of α-alumina at pH 5 and 6.

(5) Activation energy for adsorption of phthalate on α-alumina is 1.2 times less than that of benzoate–α-alumina system and the negative Gibbs free energy indicate that the adsorption of phthalate is more favourable on α-alumina than benzoate.

(6) The results imply that the adsorption of phthalate on α-alumina under similar experimental condition is more easy and favourable due to the presence of one adjacent $-COOH$ group in phthalate.

(7) Shifting of $\nu_{as}(-COO^-)$ and $\nu_s(-COO^-)$ for adsorbed benzoate and phthalate at pH 5 and 6 and appearance of a peak corresponding to $>\!C\!=\!O$ for phthalate at pH 8 suggest that:
   (a) benzoate is chemisorbed on the α-alumina surfaces resulting in outer-sphere surface complexes;
   (b) phthalate forms both outer- and inner-sphere complexes with the α-alumina surfaces. The induced solubility of α-alumina by NaCl in presence of phthalate and relative intense peak at $1418\,\mathrm{cm^{-1}}$ over $1400\,\mathrm{cm^{-1}}$ suggests that the inner-sphere complex dominates over the outer-sphere complex.

Acknowledgements

References

[1] E. Tombácz, in: S. Barany (Ed.), Role of Interfaces in Environmental Protection, Kluwer Academic Press, Amsterdam, 2003, p. 397.

[2] E.B. Cornelius, T.H. Milliken, G.A. Mills, A.G. Oblad, J. Phys. Chem. 59 (1955) 809.

[3] B. Kasprzyk-Hordern, Adv. Colloid Interface Sci. 110 (2004) 19.

[4] J.W. Elam, C.E. Nelson, M.A. Cameron, M.A. Tolbert, S.M. George, J. Phys. Chem. B 102 (1998) 7008.

[5] E. Laiti, P. Persson, L.-O. Öhman, Langmuir 14 (1998) 825.

[6] D.H. Lee, R.A. Condrate Sr., Mater. Lett. 23 (1995) 241.

[7] G.R. Aiken, D.M. McKnight, R.L. Wershaw, P. MacCarthy, Humic Substances in Soil, Sediment and Water, Interscience, NY, 1985.

[8] M.H.B. Hayes, P. MacCarthy, R.L. Malcolm, R.S. Swift (Eds.), Humic Substances I. Search of Structure, UK, 1989.

[9] R. Beckett, Surface and Colloid Chemistry in Natural Waters and Water Treatment, Plenum Press, USA, 1990.

[10] S. Mahiuddin, S. Bondopadhyay, J.N. Baruah, Int. J. Miner. Process. 26 (1989) 285.

[11] S. Mahiuddin, I. Suryanarayan, N.N. Dutta, P.C. Borthakur, Colloids Surf. 64 (1992) 177.

[12] F.-J. Göbbles, W. Püttmann, Water Res. 31 (1997) 1609.

[13] G. Plancque, B. Amekraz, V. Moulin, P. Toulhoat, C. Moulin, Rapid Commun. Mass Spectrom. 15 (2001) 827.

[14] C.R. Evanko, D.A. Dzombak, Environ. Sci. Technol. 32 (1998) 2846.

[15] C.R. Evanko, D.A. Dzombak, J. Colloid Interface Sci. 214 (1999) 189.

[16] R. Kummert, W. Stumm, J. Colloid Interface Sci. 75 (1980) 373.

[17] F. Thomas, E. Schouller, J.Y. Bottero, Colloids Surf. A. Physicochem. Eng. Aspects 95 (1995) 271.

[18] J.-F. Boily, J.B. Fein, Chem. Geol. 148 (1998) 157.

[19] M. Szekeres, E. Tombácz, K. Ferencz, I. Dékány, Colloids Surf. A. Physicochem. Eng. Aspects 141 (1998) 319.

[20] E. Molis, O. Barres, H. Marchand, E. Sauzéat, B. Humbert, F. Thomas, Colloids Surf. A. Physicochem. Eng. Aspects 163 (2000) 283.

[21] K.D. Dobson, J. McQuillan, Spectrochim. Acta Part A 56 (2000) 557.

[22] J. Rosenqvist, K. Axe, S. Sjöberg, P. Persson, Colloids Surf. A. Physicochem. Eng. Aspects 220 (2003) 91.

[23] N. Phambu, Appl. Spectrosc. 56 (2002) 756.

[24] P. Persson, J. Nordin, J. Rosenqvist, L. Lövgren, L.-O. Öhman, S. Sjöberg, J. Colloid Interface Sci. 206 (1998) 252.

[25] J. Nordin, P. Persson, E. Laiti, S. Sjöberg, Langmuir 13 (1997) 4085.

[26] O. Klug, W. Forsling, Langmuir 15 (1999) 6961.

[27] M.R. Das, O.P. Sahu, P.C. Borthakur, S. Mahiuddin, Colloids Surf. A. Physicochem. Eng. Aspects 237 (2004) 23.

[28] E. Tombácz, A. Dobos, M. Szekeres, H.D. Narres, E. Klumpp, I. Dékány, Colloid Polym. Sci. 278 (2000) 337.

[29] K. Vermöhlem, H. Lewandowski, H.-D. Narres, M.J. Schwuger, Colloids Surf. A. Physicochem. Eng. Aspects 163 (2000) 45.

[30] B. Gu, J. Schmitt, Z. Chen, L. Liang, J.F. McCarthy, Geochim. Cosmochim. Acta 59 (1995) 219.

[31] C.A. Koutstaal, V. Ponec, Appl. Surf. Sci. 70/71 (1993) 206.

[32] M.R. Das, D. Bordoloi, P.C. Borthakur, S. Mahiuddin, Colloids Surf. A. Physicochem. Eng. Aspects 254 (2005) 49.

[33] E. Tombácz, Z. Libor, E. Illés, Majzik, E. Klumpp, Org. Geochem. 35 (2004) 257.

[34] G.A. Park, Chem. Rev. 65 (1965) 177.

[35] G.V. Franks, L. Meagher, Colloids Surf. A. Physicochem. Eng. Aspects 214 (2003) 99.

[36] M. Kosmulski, J. Colloid Interface Sci. 275 (2004) 214.

[37] L. Cromières, V. Moulin, B. Fourest, E. Giffaut, Colloids Surf. A. Physicochem. Eng. Aspects 202 (2002) 101.

[38] H. Hohl, W. Stumm, J. Colloid Interface Sci. 55 (1976) 281.

[39] S.B. Johnson, T.H. Yoon, B.D. Kocar, G.E. Brown Jr., Langmuir 20 (2004) 4996.

[40] A.K. Bajpai, J. Appl. Polym. Sci. 51 (1994) 651.

[41] D.A. Dzombak, F.M.M. Morel, Surface Complexation Modelling: Hydrous Ferric Oxide, Wiley-Interscience, New York, 1990.

[42] J.P. Icenhower, P.M. Dove, Geochim. Cosmochim. Acta 64 (2000) 4193.

[43] W. Stumm, Colloids Surf. A. Physicochem. Eng. Aspects 120 (1997) 143.

[44] R.P. Groff, J. Catal. 79 (1983) 259.

[45] K. Nakamoto, Infrared Spectra of Inorganic and Co-ordination Compound, Wiley, 1963.

[46] N. Nilsson, P. Persson, L. Lövgren, S. Sjöberg, Geochim. Cosmochim. Acta 60 (1996) 4385.

[47] G. Bondietti, J. Sinniger, W. Stumm, Colloids Surf. A. Physicochem. Eng. Aspects 79 (1993) 157.

[48] W. Stumm, Aquat. Sci. 55 (1993) 273.

[49] M.V. Biber, M.D. Afonso, W. Stumm, Geochim. Cosmochim. Acta 58 (1994) 1999.

[50] M.I. Tejedor-Tejedor, E.C. Yost, M.A. Anderson, Langmuir 6 (1990) 979.